



# Dilatancy Phenomenon Study in Remolded Clays – A Micro-Macro Investigation

Qian-Feng Gao<sup>1</sup>(✉), Mohamad Jrad<sup>1</sup>, Lamine Ighil Ameu<sup>1</sup>,  
Mahdia Hattab<sup>1</sup>, and Jean-Marie Fleureau<sup>2</sup>

<sup>1</sup> Laboratoire d'Etude des Microstructures et de Mécanique des Matériaux,  
CNRS, UMR 7239, Université de Lorraine, Metz, France  
qianfeng.gao@univ-lorraine.fr

<sup>2</sup> Laboratoire de Mécanique des Sols, Structures et Matériaux, CNRS,  
UMR 8579, Université Paris-Saclay, CentraleSupélec, Gif-sur-Yvette, France

**Abstract.** The aim of this study is to analyze the influence of stress path on the dilatancy behavior of clays. Triaxial tests were conducted on saturated, remolded clay specimens. During triaxial loading, two different stress paths were considered to bring the stress level to a given point in the ( $p' - q$ ) plane. After triaxial testing, scanning electron microscopy (SEM) observations and X-ray microtomography (XR- $\mu$ CT) scans were performed on subsamples. The obtained images were processed using different software and thus the geometric characteristics of pores and cracks were identified. The microstructural characteristics were linked to the dilatancy phenomenon of specimens. The results indicate that dilatancy is influenced by stress path and may be attributed to the evolution of pore geometry and the presence of local open cracks in highly over-consolidated (OC) clays.

**Keywords:** Clays · Dilatancy · Stress path · Pore orientation  
Cracks

## 1 Introduction

Dilatancy is a typical property of clay during shearing. Normally consolidated (NC) or slightly over-consolidated (OC) clay exhibits contractancy; highly OC clay shows dilatancy. Previous work has shown that the dilatancy behavior of clay depends on the overconsolidation ratio (OCR) value, stress ratio ( $\eta = q/p'$ ) and Lode angle [1–4]. Meanwhile, the influence of the stress path on dilatancy should be emphasized. In addition, many experimental studies have revealed that the macroscopic behavior of clay is related to the evolution of its microstructure [5–8]. This makes it possible to give new insight into the dilatancy phenomenon by microscopic studies.

The aim of this research is to examine if stress path has an influence on the dilatancy phenomenon of clays. The dilatancy is approached at two different scales, the macroscale and the microscale. The experimental procedure consists in performing triaxial tests on clay specimens, then carrying out microstructural observations using scanning electron microscopy (SEM) and X-ray microtomography (XR- $\mu$ CT). The results were analyzed to link the dilatancy behavior with the microscopic phenomena.

## 2 Materials and Methodology

The studied material is an industrial kaolin clay named Kaolin K13. Its basic properties are: specific gravity  $G_s = 2.63$ , liquid limit  $w_L = 42\%$ , plastic limit  $w_P = 20\%$  and specific surface area  $s = 27 \text{ m}^2/\text{g}$ .

Four consolidated drained (CD) triaxial tests were performed on saturated remolded clay specimens (Table 1). Two tests concern the NC clay and the others concern the OC clay ( $\text{OCR} = p'_0/p'_1$ ). Two different stress paths, i.e., the constant  $\sigma'_3$  stress path (S) and the constant  $p'$  stress path (P) were considered for the triaxial shearing stage. All triaxial stress paths were stopped when stress levels approached the fixed P2 point ( $p'_2 = 300 \text{ kPa}$ ,  $q_2 = 150 \text{ kPa}$ ) in the  $(p', q)$  plan (Fig. 1).

**Table 1.** Triaxial tests on saturated remolded clay.

Specimen	OCR	Stress path	$p'_0$ (kPa)	$p'_1$ (kPa)
NC_S250_P2	1.0	S	250	–
OCR4.0_S250_P2	4.0	S	1000	250
NC_P300_P2	1.0	P	300	–
OCR3.3_P300_P2	3.3	P	1000	300

Notes:  $p'_0$  and  $p'_1$  are the isotropic effective stresses for NC clay and OC clay, respectively.

After triaxial loading, specimens were recovered and then cut into subsamples for SEM observations and XR- $\mu$ CT scans. ImageJ and Avizo software were then used to process and analyze the clay microstructure (i.e., pores and cracks).

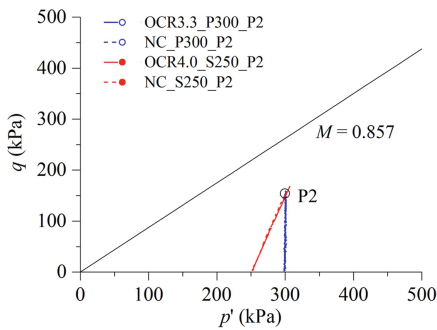


**Fig. 1.** Two different stress paths.

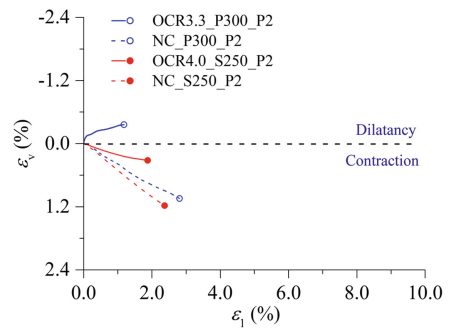


**Fig. 2.** Evolution of volumetric strain.

### 3 Results and Discussion

#### 3.1 Macroscopic Behavior

Figure 2 shows the volumetric behavior of the specimens under different loading conditions. One can note that the two NC specimens are contractive regardless of stress paths. Nevertheless, the two OC specimens exhibit two different volumetric behaviors. The specimen (OCR4.0\_S250\_P2) under constant  $\sigma'_3$  stress path shows contractive behavior, while the specimen (OCR3.3\_P300\_P2) under the constant  $p'$  stress path shows dilatant behavior. These results indicate that the dilatancy phenomenon is affected by stress paths.

#### 3.2 Pore Shape and Pore Orientation

The pore roundness ( $R_s$  = ratio of the minor axis to the major axis) and the pore orientation ( $\theta$  = angle of the major axis with respect to the horizontal plane) were analyzed.

The pore roundness curves in Fig. 3a are characterized by a unimodal distribution for all specimens under triaxial loading. Moreover, compared to the contractive specimens, the curve of the dilatant specimen (OCR3.3\_P300\_P2) presents a wider peak shifted to the right, which corresponds to more open pores.

The pore orientation curves in Fig. 3b are away from the depolarization (D) line (that represents a perfectly random orientation) and show preferential orientation of pores. Furthermore, the curve of the dilatant specimen (OCR3.3\_P300\_P2) is relatively close to the D line, which means that the pores tend toward a random orientation.

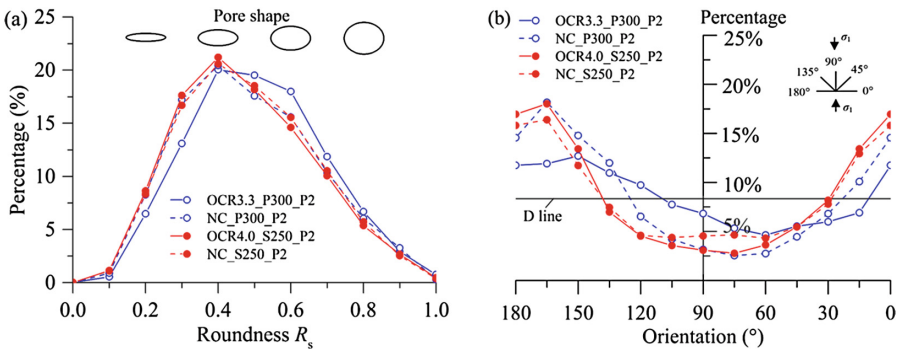


Fig. 3. Micropore structure: (a) pore roundness; (b) pore orientation.

#### 3.3 Micro- and Meso-Cracks

From SEM images (Fig. 4a, b), we can notice the appearance of micro-cracks between weakly-linked and parallel-oriented particle groups in both NC and OC specimens. These micro-cracks have lengths varying from around 5  $\mu\text{m}$  to 15  $\mu\text{m}$  and small

thicknesses of 0.5–1.0  $\mu\text{m}$ . However, several open meso-cracks (whose lengths are larger than 100  $\mu\text{m}$ ) with tortuous surfaces are found only in specimen OCR3.3\_P300\_P2 (Fig. 4c). It seems that the activation of open meso-cracks is due to the propagation of micro-cracks and closely related to the dilatancy phenomenon. Notice that meso-cracks may also exist in contractive specimens, but they are probably closed and cannot be detected with XR- $\mu\text{CT}$ .

From the above analyses, one can note the strong relationship observed between the dilatancy phenomenon and the microstructure of clay. The results show that in highly OC clay, dilatancy develops owing to the increasing opening of pores associated with a random pore orientation. During loading, along the stress path, these pores lead to open microcracks that can propagate up to the mesoscopic level.

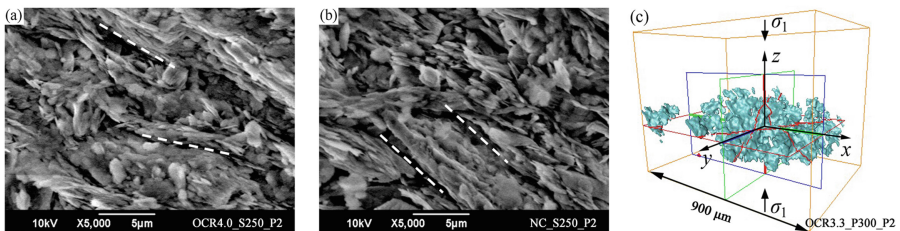


**Fig. 4.** Micro-cracks in (a) OCR4.0\_S250\_P2 and (b) NC\_S250\_P2; and meso-cracks in (c) OCR3.3\_P300\_P2.

## 4 Conclusions

The following conclusions can be drawn from this study: (i) for a given stress level, the dilatancy phenomenon is clearly affected by stress paths; (ii) the dilatancy development may be attributed to the evolution of pore geometry, and the formation of local open cracks.

**Acknowledgement.** We would like to acknowledge the scholarship offered by China Scholarship Council (CSC) for the first author's Ph.D study.

## References

1. Ye, G.L., Ye, B., Zhang, F.: Strength and dilatancy of overconsolidated clays in drained true triaxial tests. *J. Geotech. Geoenviron. Eng.* **140**(4), 06013006 (2014)
2. Hattab, M., Hicher, P.Y.: Dilating behaviour of overconsolidated clay. *Soils Found.* **44**(4), 27–40 (2004)
3. Shimizu, M.: Effect of overconsolidation on dilatancy of a cohesive soil. *Soils Found.* **22**(4), 121–135 (1982)
4. Matsuoka, H.: Dilatancy characteristics of soil. *Soils Found.* **14**(3), 13–24 (1974)

5. Hattab, M., Hammad, T., Fleureau, J.M.: Internal friction angle variation in a kaolin/montmorillonite clay mix and microstructural identification. *Géotechnique* **65**(1), 1–11 (2015)
6. Hattab, M., Fleureau, J.M.: Experimental analysis of kaolinite particle orientation during triaxial path. *Int. J. Numer. Anal. Methods Geomech.* **35**(8), 947–968 (2011)
7. Hattab, M., Fleureau, J.M.: Experimental study of kaolin particle orientation mechanism. *Géotechnique* **60**(5), 323–331 (2010)
8. Li, X., Zhang, L.M.: Characterization of dual-structure pore-size distribution of soil. *Can. Geotech. J.* **46**(2), 129–141 (2009)